Event-triggered Neural Network Control using Quadratic Constraints for Perturbed Systems

Carla de Souza, Antoine Girard, Sophie Tarbouriech

▶ **To cite this version:**

Carla de Souza, Antoine Girard, Sophie Tarbouriech. Event-triggered Neural Network Control using Quadratic Constraints for Perturbed Systems. Automatica, 2023, 157, pp.111237. 10.1016/j.automatica.2023.111237 . hal-04154871

HAL Id: hal-04154871
https://hal.science/hal-04154871

Submitted on 7 Jul 2023

HAL is a multi-disciplinary open access archive for the deposit and dissemination of scientific research documents, whether they are published or not. The documents may come from teaching and research institutions in France or abroad, or from public or private research centers.

L'archive ouverte pluridisciplinaire **HAL**, est destinée au dépôt et à la diffusion de documents scientifiques de niveau recherche, publiés ou non, émanant des établissements d'enseignement et de recherche français ou étrangers, des laboratoires publics ou privés.

Event-triggered Neural Network Control using Quadratic Constraints for Perturbed Systems ⋆

Carla de Souza [a], Antoine Girard [b], Sophie Tarbouriech [a]

[a] *LAAS-CNRS, Université de Toulouse, CNRS, Toulouse, France.*

[b] *Université Paris-Saclay, CNRS, CentraleSupélec, Laboratoire des signaux et systèmes, 91190, Gif-sur-Yvette, France.*

Abstract

This paper investigates the event-triggered control problem for perturbed systems under neural network controllers. We propose a novel event-triggering mechanism, based on local sector conditions related to the activation functions, to reduce the computational cost associated with the neural network evaluation. It avoids redundant computations by updating only a portion of the layers instead of evaluating periodically the whole neural network. Sufficient conditions in terms of matrix inequalities are established to design the parameters of the event-triggering mechanism and compute an inner-approximation of the region of attraction for the perturbed feedback system. The theoretical conditions are obtained by using a quadratic Lyapunov function and an abstraction of the activation functions via quadratic constraints to decide whether the outputs of the layers should be transmitted through the network or not. Such conditions allow us to reduce the computational activity on the neural network while preserving the stability and performance level of the perturbed feedback system. To illustrate the efficacy of our approach, we consider the nonlinear inverted pendulum system stabilized by a trained neural network.

Key words: Emulation; Event-triggering mechanisms; Neural network control; Quadratic constraints;

1 Introduction

Due to the recent advancements in deep learning, there has been an increasing interest in using neural networks (NNs) to stabilize dynamic systems. For example, NNs have been used to replace existing computationally expensive controllers such as model predictive controllers (MPCs), which require online solutions to an optimal control problem. In that way, they allow for an efficient and inexpensive embedded implementation [13,34,16]. Despite their high performance, NN controllers lack guarantees, which typically restrict their use in safety-critical applications such as autonomous driving, robots for surgical procedures, and medical support systems. Therefore, it is crucial to develop tools that can provide useful certificates of stability, safety, and robustness for NN controlled systems. Motivated by this, several works have studied the challenging task of verifying such systems. [7] certifies tight bounds on the Lipschitz constant of deep NNs, which is a common proxy for robustness. [22,20] also enforce accurate Lipschitz bounds, but during training. For stability analysis, sufficient conditions based on linear matrix inequalities (LMIs) are derived by abstracting the nonlinear activation function in NNs through Quadratic Constraints (QC) [18] or by linear difference inclusions (LDIs) [26]. Similar QCs abstractions are proposed by [33] to analyze perturbed plants with perturbations described by integral quadratic constraints (IQCs). As an extension, [21] analyzes stability in offset-free setpoint tracking with a piecewise constant reference. Both approaches provide ellipsoidal inner approximations of the corresponding regions of attraction. [15] formulates QCs based on partial gradients to certify the input-output stability of reinforcement-learning (RL) controlled systems. Therefore, the use of QCs in this context has been shown to be effective.

Different from traditional control systems, network control systems not only need to provide satisfactory control requirements in terms of stability and safety but also need to consider the usage of network resources [12]. To reduce communication traffic and save computational burden on the processors, an alternate control paradigm entitled event-triggered control (ETC) emerged [25]. In this strategy, the sporadic execution of control tasks is determined by some well-

⋆ Research funded by ANR via project HANDY, number ANR-18-CE40-0010.

Email addresses: carla.souza93@hotmail.com (Carla de Souza), antoine.girard@l2s.centralesupelec.fr (Antoine Girard), tarbour@laas.fr (Sophie Tarbouriech).

designed event-triggering mechanism (ETM), rather than the elapse of a scheduled time sequence. As a consequence, the ETC is capable of reducing the execution rate of control tasks while guaranteeing suitable properties for the system. Recently, various mechanisms have been proposed for various systems in the literature [4,11,32,1]. In the context of neural networks, the event-triggering technique has been used mostly to transmit states during the learning process. [23] investigates the approximation-based ETC for multi-input multi-output continuous-time unknown affine nonlinear systems, where the controller is approximated via a linearly parameterized neural network. The event-triggered manner has also been combined with intelligent algorithms to solve optimal control problems. [28] proposes an adaptive event-triggering algorithm based on the actor-critic structure for continuous-time nonlinear systems. A similar approach is developed in [35] for nonlinear systems with unknown dynamics. Based on the universal approximator [30], i.e. the three-layer fully connected feed-forward neural network (FCDNN), [9] designs a four-layer FCDNN based event-triggering controller for continuous-time nonlinear systems. The genetic algorithm (GA) is used to optimize the initial weights and thresholds, thus reducing the controller error. However, to the best of the authors knowledge, the event-triggering scheme has not yet been used to update the layers outputs in a scenario where the controller is known, thus saving computational resources.

According to the discussion above, the paper aims at filling such a gap by providing the following features: *i)* the design of an ETM to update only a portion of the neural network layers directly related to the activation functions, thus reducing the computational cost associated with the evaluation of the control law; *ii)* the development of sufficient convex-conditions that allow us to compute the triggering parameters and to characterize an estimate of the region of attraction for the perturbed feedback system while ensuring its stability and suitable performance. Different from the triggering policies commonly investigated in the literature, we employ local sector conditions satisfied by the activation functions to decide whether the outputs of the layers should be transmitted through the network or not. We use quadratic constraints (QCs) not only to abstract the nonlinear activation functions but also to model the event-triggering rule. As usual, Integral Quadratic Constraints (IQCs) allow to capture the perturbation's input/output behavior. Note that the approach proposed differs from that of [33] in two main aspects: 1) our analysis with perturbed plants and NN controller is based on QCs with more general multipliers; 2) we design ETMs based on the QCs to reduce the computational cost associated with the control law evaluation. Thanks to the use of quadratic Lyapunov function, the theoretical conditions are formulated as matrix inequalities, which can be made linear provided that some parameters are fixed. An optimization procedure is proposed in order to deal with the classical trade-off between update saving and size of the inner approximation of the region of attraction of the equilibrium point. The current paper can be viewed as complementary to [3] as summarized as follows: we consider 1) general activation function instead of saturation; 2) QC based ETM instead of more classical error based ETM; 3) perturbed systems instead of linear ones.

The paper is organized as follows. Section 2 describes the complete model under consideration and the way to abstract the activation function for stability purposes. Section 3 states the proposed event-triggering strategy based on quadratic abstraction and formulates the main theoretical conditions, which allows us to compute the triggering parameters and an inner-approximation of the region of attraction for the perturbed feedback system. Illustrations are provided in Section 4 by considering the inverted pendulum considered in [33]. Finally, Section 5 points out some concluding remarks and potential future works.

Notation. $\mathbb{N}$, $\mathbb{R}^n$, $\mathbb{R}^{n\times m}$ denote the sets of nonnegative integers, n-dimensional vectors and $n \times m$ matrices, respectively. Given two vectors $v, w \in \mathbb{R}^n$, $v \leq w$ if $v_i \leq w_i$, for all $i = 1, \ldots, n$. Then, $[v, w]$ is the set of vectors u such that $v \leq u \leq w$. For any matrix A, $A^\top$ denotes its transpose. Given two symmetric matrices $A, B \in \mathbb{R}^{n\times n}$, $A \leq B$ (resp. $A < B$) stands for $B - A$ being positive semi-definite (resp. positive definite). For $v \in \mathbb{R}^n$, $\texttt{diag}(v)$ denotes the diagonal matrix whose diagonal elements are given by the coordinates of v. For v_1, v_2, $\texttt{diag}([v_1, v_2])$ denote the set of diagonal matrices D such that $\texttt{diag}(v_1) \leq D \leq \texttt{diag}(v_2)$. $\texttt{bdiag}(A_1, \ldots, A_n)$ is a block diagonal matrix with matrices $A_1, \ldots, A_n$ on the diagonal. $\mathbf{I}$ and $\mathbf{0}$ stand respectively for the identity and the null matrix of appropriate dimensions. $\mathbf{1}$ denotes a vector of ones of appropriate dimension. For a partitioned matrix, the symbol $\star$ stands for symmetric blocks. $\mathbb{RL}_\infty$ is the set of rational functions with real coefficients and no poles on the unit circle. $\mathbb{RH}_\infty \subset \mathbb{RL}_\infty$ contains functions that are analytic in the closed exterior of the unit disk in the complex plane. $\ell_2^{n_x}$ is the set of sequences $x : \mathbb{N} \to \mathbb{R}^{n_x}$ with $\|x\|_2 = \sqrt{\sum_{k=0}^{\infty} x(k)^\top x(k)}$. The shorthand expression $[\bullet]^\top \Pi x$ denotes $x^\top \Pi x$ to save place.

2 Modelling and Problem Statement

2.1 Model Description

Consider the perturbed feedback system illustrated in Figure 1, which is composed by a perturbed plant $\mathbb{G}(G, \Delta)$ and an event-triggered neural network controller π_{ETM}. The perturbed plant is an interconnection of a nominal linear plant G and a nonlinear perturbation Δ. To reduce the computational cost associated

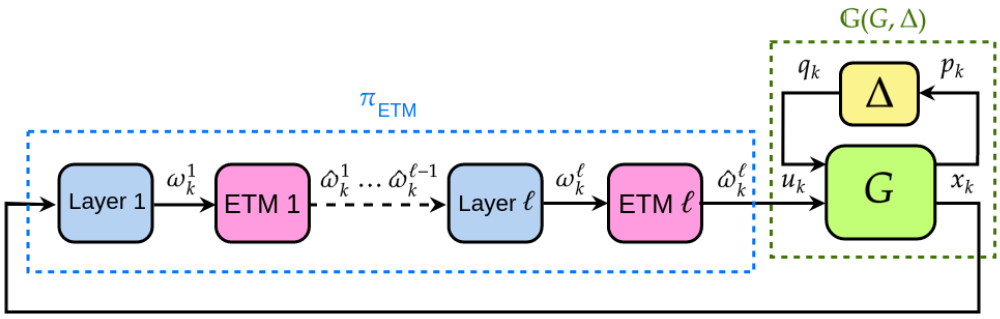

Fig. 1. The perturbed feedback system $\mathbb{G}(G,\Delta)$ and event triggered neural network controller π_{ETM}.

with the evaluation of the control law, ETMs are introduced after each layer of the neural network. They decide whether or not the output of a layer should be transmitted to subsequent layers of the neural network. Such a scheme aims at significantly reducing the update rate of the layers, while preserving the system stability. Another possibility could be to use an ETM after each neuron. The approach developed in this work can be extended to this case with mild modifications.

The nominal plant G is described by the following linear equations:

$$\begin{aligned} x(k+1) &= A_G x(k) + B_{Gu} u(k) + B_{Gq} q(k), \\ p(k) &= C_G x(k) + D_{Gu} u(k) + D_{Gq} q(k), \end{aligned} \tag{1}$$

where $x(k) \in \mathbb{R}^{n_G}$ is the state vector, $u(k) \in \mathbb{R}^{n_u}$ is the control input, and $p(k) \in \mathbb{R}^{n_p}$ and $q(k) \in \mathbb{R}^{n_q}$ are the input and output of the perturbation Δ, respectively. The interconnection between G and Δ is set up through the constraint:

$$q(\cdot) = \Delta(p(\cdot)). \tag{2}$$

where Δ is assumed to be a bounded, causal operator, i.e. $\Delta : \ell_2^{n_p} \to \ell_2^{n_q}$. The precise type of perturbation Δ that we consider will be formally defined in the next subsection.

The controller π_{ETM} is an ℓ-layer, feedforward event-triggered neural network (NN) defined, for all $i \in \{1, \dots, \ell\}$, by:

$$\begin{aligned} \hat{\omega}^0(k) &= x(k), \\ \nu^i(k) &= W^i \hat{\omega}^{i-1}(k) + b^i, \\ \omega^i(k) &= \phi^i(\nu^i(k)), \\ u(k) &= W^{l+1} \hat{\omega}^\ell(k) + b^{\ell+1}, \end{aligned} \tag{3}$$

where $\nu^i(k) \in \mathbb{R}^{n_i}$ is the input to the i^{th} activation function, and $\omega^i(k) \in \mathbb{R}^{n_i}$ and $\hat{\omega}^i(k) \in \mathbb{R}^{n_i}$ are the current output and the last transmitted output from the i^{th} layer, respectively. The operations for each layer are defined by a weight matrix $W^i \in \mathbb{R}^{n_i \times n_{i-1}}$, a bias vector $b^i \in \mathbb{R}^{n_i}$, and a nonlinear activation function $\phi^i : \mathbb{R}^{n_i} \to \mathbb{R}^{n_i}$. The activation function is applied element-wise, i.e.

$$\phi^i(\nu^i) = \begin{bmatrix} \varphi(\nu_1^i) & \dots & \varphi(\nu_{n_i}^i) \end{bmatrix}^\top, \tag{4}$$

where $\varphi : \mathbb{R} \to \mathbb{R}$ is the (scalar) activation function of each neuron. For simplicity, they are assumed identical in all layers. Gather the inputs and outputs of all activation functions into augmented vectors as:

$$\nu_\phi = \begin{bmatrix} \nu^1 \\ \vdots \\ \nu^\ell \end{bmatrix}, \ \omega_\phi = \begin{bmatrix} \omega^1 \\ \vdots \\ \omega^\ell \end{bmatrix}, \ \hat{\omega}_\phi = \begin{bmatrix} \hat{\omega}^1 \\ \vdots \\ \hat{\omega}^\ell \end{bmatrix} \in \mathbb{R}^{n_\phi}, \tag{5}$$

where $n_\phi = \sum_{i=1}^{\ell} n_i$. Then, stack all activation functions to define the combined nonlinearity $\phi : \mathbb{R}^{n_\phi} \to \mathbb{R}^{n_\phi}$ as:

$$\phi(\nu_\phi) = \begin{bmatrix} \phi^1(\nu^1)^\top & \dots & \phi^\ell(\nu^\ell)^\top \end{bmatrix}^\top, \tag{6}$$

thus

$$\omega_\phi(k) = \phi(\nu_\phi(k)), \tag{7}$$

where the (scalar) activation function is applied element-wise to each entry of ν_ϕ. Finally, in the same spirit as in [33,6] the NN control policy defined in (3) can be rewritten as:

$$\begin{bmatrix} u(k) \\ \nu_\phi(k) \end{bmatrix} = N \begin{bmatrix} x(k) \\ \hat{\omega}_\phi(k) \\ 1 \end{bmatrix}, \tag{8}$$

where

$$N = \left[\begin{array}{ccccc|c} \mathbf{0} & \mathbf{0} & \dots & \mathbf{0} & W^{\ell+1} & b^{\ell+1} \\ \hline W^1 & \mathbf{0} & \dots & \mathbf{0} & \mathbf{0} & b^1 \\ \mathbf{0} & W^2 & \dots & \mathbf{0} & \mathbf{0} & b^2 \\ \vdots & \vdots & \ddots & \vdots & \vdots & \vdots \\ \mathbf{0} & \mathbf{0} & \dots & W^\ell & \mathbf{0} & b^\ell \end{array}\right] = \left[\begin{array}{c|c|c} N_{ux} & N_{u\omega} & N_{ub} \\ \hline N_{\nu x} & N_{\nu\omega} & N_{\nu b} \end{array}\right].$$

Such a decomposition isolates the activation functions allowing us to describe the closed loop through relations (1), (2), (7) and (8). The relation between the current and transmitted outputs $\omega_\phi(k)$ and $\hat{\omega}_\phi(k)$ is described by an ETM that will be formally introduced in Section 3. Finally, we assume that (1), (2), (7), (8) admit a steady state $(x_*, u_*, \nu_*, \omega_*, \hat{\omega}_*, p_*, q_*)$ where $\omega_* = \hat{\omega}_*$, $p_* = 0$ and $q_* = 0$.

2.2 Perturbation as Integral Quadratic Constraints

The perturbation Δ is modeled as an operator mapping inputs to outputs, which can be characterized by an integral quadratic constraint (IQC), consisting of a "virtual" filter Ψ applied to the input $p(\cdot)$ and output $q(\cdot)$ of Δ and a constraint on the output of Ψ. Such a filter Ψ is defined by the following equations:

$$\begin{aligned} \psi(k+1) &= A_\Psi \psi(k) + B_{\Psi p} p(k) + B_{\Psi q} q(k), \\ r(k) &= C_\Psi \psi(k) + D_{\Psi p} p(k) + D_{\Psi q} q(k), \end{aligned} \tag{9}$$

where $\psi(k) \in \mathbb{R}^{n_\psi}$, with $\psi(0) = 0$, is the state vector, $r(k) \in \mathbb{R}^{n_r}$ is the output signal, and A_Ψ is a Schur matrix with appropriate dimensions. In the following we will use the shorthand expression to define the filter (9):

$$\Psi = \left[\begin{array}{c|cc} A_\Psi & B_{\Psi p} & B_{\Psi q} \\ \hline C_\Psi & D_{\Psi p} & D_{\Psi q} \end{array}\right] \tag{10}$$

IQCs can be expressed in both the frequency and time domain. Time domain IQCs consist of hard IQCs and soft IQCs, which are quadratic constraints on r over finite and infinite horizons, respectively [19,24,29,14]. In this work, we focus on the analysis with hard IQCs. Note that the hard IQCs framework allows to deal with different purposes as the fact to handle nonlinearities, time variations as delay, uncertain parameters or unmodeled dynamics.

Definition 1 (Hard IQCs) *Let the matrices Ψ as defined in (10), $\Psi \in \mathbb{RH}_\infty^{n_r \times (n_p + n_q)}$ and $M = M^\top \in \mathbb{R}^{n_r}$ be given. The bounded, causal operator $\Delta : \ell_2^{n_p} \to \ell_2^{n_q}$ satisfies the hard IQC defined by (Ψ, M) if for all $p(\cdot) \in \ell_2^{n_p}$, $q(\cdot) = \Delta(p(\cdot))$ and for all $N \geq 0$, the following inequality holds*

$$\sum_{k=0}^{N} r(k)^\top M r(k) \geq 0. \tag{11}$$

Thus, relation (2) can be abstracted by dynamics (9) and the constraint (11) on $r(\cdot)$. From now on, the notation $\Delta \in \mathrm{IQC}(\Psi, M)$ is used to indicate that the perturbation Δ satisfies Definition 1. Moreover, we use ψ_* to denote the value of $\psi(k)$ at the equilibrium. Note that since we assume that $p_* = 0$ and $q_* = 0$, we have $\psi_* = 0$.

2.3 Activation Functions as Quadratic Constraints

In order to develop conditions to design the event-triggering strategy and to ensure the closed-loop stability, we need to provide some abstraction to deal with the activation functions. Inspired by [27], [33], the way chosen to embed the nonlinearities is a set of quadratic constraints (QCs). The most famous one is the classical sector condition recalled in the definition below.

Definition 2 (Local sector condition [17]) *Let α, β, $\underline{v}$, $\bar{v}$, $v_* \in \mathbb{R}$ with $\alpha \leq \beta$ and $\underline{v} \leq v_* \leq \bar{v}$. The function $\varphi : \mathbb{R} \to \mathbb{R}$ satisfies the local sector $\mathrm{sec}[\alpha, \beta]$ around the point v_* restricted to the interval $[-\bar{v}, \bar{v}]$ if the following condition holds for all $v \in [\underline{v}, \bar{v}]$:*

$$(\varphi(v) - \varphi(v_*) - \alpha(v - v_*))(\varphi(v) - \varphi(v_*) - \beta(v - v_*)) \leq 0. \tag{12}$$

As an example, $\varphi(v) = \tanh(v)$ satisfies the local sector $\mathrm{sec}[\alpha, \beta]$ around the point $v_* = 0$ restricted to the interval $[-\bar{v}, \bar{v}]$ with $\alpha = \frac{\tanh(\bar{v})}{\bar{v}}$ and $\beta = 1$. The local sector constraint comes from applying tighter bounds to the global sector $\mathrm{sec}[0, 1]$, which encompasses many activation functions, such as tanh, ReLU, and sigmoid.

Local sectors can also be defined for the combined nonlinearity $\phi : \mathbb{R}^{n_\phi} \to \mathbb{R}^{n_\phi}$, given by (6), around the equilibrium value ν_*. For α_ϕ, β_ϕ, $\underline{\nu}$, $\bar{\nu}$, with $\alpha_\phi \leq \beta_\phi$ and $\underline{\nu} \leq \nu_* \leq \bar{\nu}$, we say that ϕ satisfies the local sector $\mathrm{sec}[\alpha_\phi, \beta_\phi]$ around the point ν_* restricted to the interval $[\underline{\nu}, \bar{\nu}]$ if each function $\omega_{\phi,i} = \varphi(\nu_{\phi,i})$ satisfies the local sector $\mathrm{sec}[\alpha_i, \beta_i]$ around the point $\nu_{*,i}$ restricted to $\nu_{\phi,i} \in [\underline{\nu}_i, \bar{\nu}_i]$.

Remark 1 *To choose interval bounds $\underline{\nu}, \bar{\nu} \in \mathbb{R}^{n_\phi}$ that are consistent with our neural network, we proceed as follows. Consider the equilibrium value at the first layer ν_*^1 and select $\underline{\nu}^1$, $\bar{\nu}^1 \in \mathbb{R}^{n_1}$ such that $\underline{\nu}^1 \leq \nu_*^1 \leq \bar{\nu}^1$. Then, compute the bounds of the output ω^1, i.e. $\underline{\omega}^1$, $\bar{\omega}^1 \in \mathbb{R}^{n_1}$, from the equality $\omega^1 = \phi^1(\nu^1)$. The latter, in turn, allows us to compute the bounds of the next activation input ν^2, i.e. $\underline{\nu}^2$, $\bar{\nu}^2 \in \mathbb{R}^{n_2}$, from the weight matrix W^1. By propagating this process through all layers of the neural network, we are then able to obtain a suitable interval $[\underline{\nu}, \bar{\nu}]$ for the activation input ν_ϕ (see [33] for more details).* ∘

The local sector condition for nonlinearity ϕ can be rewritten in compact form as shown in the following lemma.

Lemma 1 ([33]) *Let α_ϕ, β_ϕ, $\underline{\nu}$, $\bar{\nu} \in \mathbb{R}^{n_\phi}$ be given with $\alpha_\phi \leq \beta_\phi$ and $\underline{\nu} \leq \nu_* \leq \bar{\nu}$, let $\omega_* = \phi(\nu_*)$. Assume ϕ satisfies the local sector $\mathrm{sec}[\alpha_\phi, \beta_\phi]$ around the point ν_* restricted to the interval $[\underline{\nu}, \bar{\nu}]$. Then, for any diagonal positive semi-definite matrix $T \in \mathbb{R}^{n_\phi \times n_\phi}$ and for*

all $\nu_\phi \in [\underline{\nu}, \bar{\nu}]$

$$\left[\bullet\right]^\top \underbrace{\begin{bmatrix} -2\mathtt{diag}(\alpha_\phi)\mathtt{diag}(\beta_\phi)T & \star \\ \mathtt{diag}(\alpha_\phi+\beta_\phi)T & -2T \end{bmatrix}}_{\Pi_{ds}} \begin{bmatrix} \nu_\phi - \nu_* \\ \phi(\nu_\phi) - \omega_* \end{bmatrix} \geq 0. \tag{13}$$

The matrix Π_{ds} in (13) is the so-called diagonally structured multiplier. Such a multiplier has been often used in the literature, but it may cause unnecessary conservatism when not associated with others [8]. Note however that such a multiplier actually belongs to a more general class, the polytopic bounding multipliers. The following lemma, directly adapted from [5], provides a local sector condition based on the polytopic bounding multipliers.

Lemma 2 *Let* $\alpha_\phi, \beta_\phi, \underline{\nu}, \bar{\nu} \in \mathbb{R}^{n_\phi}$ *be given with* $\alpha_\phi \leq \beta_\phi$ *and* $\underline{\nu} \leq \nu_* \leq \bar{\nu}$*, let* $\omega_* = \phi(\nu_*)$*. Assume* ϕ *satisfies the local sector* $\mathrm{sec}[\alpha_\phi, \beta_\phi]$ *around the point* ν_* *restricted to the interval* $[\underline{\nu}, \bar{\nu}]$*. Let us define the set of matrices*

$$\Pi_{pol}[\alpha_\phi, \beta_\phi] := \{\Pi = \Pi^\top \in \mathbb{R}^{2n_\phi \times 2n_\phi} : \left[\begin{smallmatrix} \mathbf{I} \\ \Lambda \end{smallmatrix}\right]^\top \Pi \left[\begin{smallmatrix} \mathbf{I} \\ \Lambda \end{smallmatrix}\right] \geq \mathbf{0}, \forall \Lambda \in \mathtt{diag}([\alpha_\phi, \beta_\phi])\}. \tag{14}$$

Then, for any $\Pi \in \Pi_{pol}[\alpha_\phi, \beta_\phi]$ *and for all* $\nu_\phi \in [\underline{\nu}, \bar{\nu}]$

$$\left[\bullet\right]^\top \Pi \begin{bmatrix} \nu_\phi - \nu_* \\ \phi(\nu_\phi) - \omega_* \end{bmatrix} \geq 0. \tag{15}$$

Let us remark that Π_{ds}, defined in Lemma 1, belongs to $\Pi_{pol}[\alpha_\phi, \beta_\phi]$. Without loss of generality, an element of $\Pi_{pol}[\alpha_\phi, \beta_\phi]$ can be written under the form

$$\Pi = \begin{bmatrix} X & Y \\ \star & Z \end{bmatrix} \tag{16}$$

where $X, Y, Z \in \mathbb{R}^{n_\phi \times n_\phi}$. As stated in [5], it is hard to check whether $\Pi \in \Pi_{pol}[\alpha_\phi, \beta_\phi]$ holds, since $\Pi_{pol}[\alpha_\phi, \beta_\phi]$ is characterized by infinitely many constraints. However, if we constrain the diagonal elements of Z to be nonpositive, it is sufficient to check the condition in (14) for all matrices Λ corresponding to the finitely many vertices of the matrix interval $\mathtt{diag}([\alpha_\phi, \beta_\phi])$.

Moreover, to account for the structure of the neural network, we constrain the matrices X, Y and Z to be block diagonal:

$$X = \mathtt{bdiag}(X_1, \ldots, X_\ell),\ Y = \mathtt{bdiag}(Y_1, \ldots, Y_\ell), \quad Z = \mathtt{bdiag}(Z_1, \ldots, Z_\ell), \tag{17}$$

where $X_i, Y_i, Z_i \in \mathbb{R}^{n_i \times n_i}$, $i = 1, \ldots, \ell$. Due to this particular structure, it follows that

$$\left[\bullet\right]^\top \Pi \begin{bmatrix} \nu_\phi - \nu_* \\ \phi(\nu_\phi) - \omega_* \end{bmatrix} = \sum_{i=1}^{\ell} \left[\bullet\right]^\top \Pi_i \begin{bmatrix} \nu^i - \nu_*^i \\ \phi^i(\nu^i) - \omega_*^i \end{bmatrix} \tag{18}$$

where for $i = 1, \ldots, \ell$,

$$\Pi_i = \begin{bmatrix} X_i & Y_i \\ \star & Z_i \end{bmatrix}.$$

Moreover, it follows from Lemma 2, that for all $\nu^i \in [\underline{\nu}^i, \bar{\nu}^i]$

$$\left[\bullet\right]^\top \Pi_i \begin{bmatrix} \nu^i - \nu_*^i \\ \phi^i(\nu^i) - \omega_*^i \end{bmatrix} \geq 0. \tag{19}$$

3 Event-Triggering Mechanism

3.1 Definition of the ETM

Since the evaluation of a function defined by a neural network can be costly, we propose event-triggering mechanisms (ETMs) enabling to compute the output of the neural network by updating only a portion of its layers instead of providing periodic sampling of all of them. In such a way, we can reduce the computational cost associated with the neural network evaluation while preserving the stability of the feedback system. In this work, differently from the standard error-based functions often used in the literature [2,10,31], we propose a new event-triggering policy, which is based on the QCs presented in Section 2.3, to decide whether or not the current outputs $\omega^i(k)$ should be transmitted through the neural network.

Let ϕ satisfies the local sector $\mathrm{sec}[\alpha_\phi, \beta_\phi]$ around the point ν_* restricted to the interval $[\underline{\nu}, \bar{\nu}]$ and let $\Pi \in \Pi_{pol}[\alpha_\phi, \beta_\phi]$ be of the form (16), (17). The ETM is given by the following rule

$$\hat{\omega}^i(k) := \begin{cases} \hat{\omega}^i(k-1), \text{ if } \left[\bullet\right]^\top \Pi_i \begin{bmatrix} \nu^i(k) - \nu_*^i \\ \hat{\omega}^i(k-1) - \omega_*^i \end{bmatrix} \geq 0. \\ \omega^i(k), \qquad \text{otherwise.} \end{cases} \tag{20}$$

for all $i = 1, \ldots, \ell$.

Lemma 3 *Let us assume that* $\nu^1(k) \in [\underline{\nu}^1, \bar{\nu}^1]$ *for all* $k \in \mathbb{N}$*. Then, the following condition is always satisfied, for all* $k \in \mathbb{N}$*,*

$$\left[\bullet\right]^\top \Pi \begin{bmatrix} \nu_\phi(k) - \nu_* \\ \hat{\omega}_\phi(k) - \omega_* \end{bmatrix} \geq 0. \tag{21}$$

Proof. First, let us remark that it follows from Remark 1 that if $\nu^1(k) \in [\underline{\nu}^1, \bar{\nu}^1]$, then $\nu_\phi(k) \in [\underline{\nu}, \bar{\nu}]$. For $i = 1, \ldots, \ell$, let us analyze the two possible cases allowed from (20) and show that

$$\begin{bmatrix}\bullet\end{bmatrix}^\top \Pi_i \begin{bmatrix}\nu^i(k) - \nu^i_* \\ \hat{\omega}^i(k) - \omega^i_*\end{bmatrix} \geq 0. \tag{22}$$

First, if the QC in (20) is satisfied, then $\hat{\omega}^i(k)$ can keep its latest value, i.e. $\hat{\omega}^i(k) = \hat{\omega}^i(k-1)$, ensuring the validity of (22). On the other hand, if the QC in (20) is not satisfied, then $\hat{\omega}^i(k)$ will receive the current output $\omega^i(k)$, i.e. $\hat{\omega}^i(k) = \omega^i(k)$, so that (22) will also be verified by (7) and (19). The proof is completed by remarking that due to the particular structure of Π given by (16) and (17) we have similarly to (18) that

$$\begin{bmatrix}\bullet\end{bmatrix}^\top \Pi \begin{bmatrix}\nu_\phi(k) - \nu_* \\ \hat{\omega}_\phi(k) - \omega_*\end{bmatrix} = \sum_{i=1}^{\ell} \begin{bmatrix}\bullet\end{bmatrix}^\top \Pi_i \begin{bmatrix}\nu^i(k) - \nu^i_* \\ \hat{\omega}^i(k) - \omega^i_*.\end{bmatrix}$$

This gives us (21). □

Remark 2 *For the proposed ETM* (20)*, it interesting to check that if at a given instant k, the layer i is not triggered, i.e. $\hat{\omega}^i(k) = \hat{\omega}^i(k-1)$, then* (3) *gives that $\nu^{i+1}(k) = \nu^{i+1}(k-1)$. Further, since* (22) *holds at time $k-1$ for layer $i+1$, we get from* (20) *that the update of layer $i+1$ will not be triggered at time k, and the same holds for all layers $i+2, \ldots, \ell$. This means that whenever the update of a layer is not triggered, the ETM of the subsequent layers does not need to be evaluated, thus saving additional computations.* ∘

In the remaining of the paper, the problem we intend to solve can be summarized as follows.

Problem 1 *Consider the NN controller π_{ETM}* (7)*-(8) that stabilizes the perturbed plant $\mathbb{G}(G, \Delta)$ (1)-(9)-(11). Design ETMs, according to (20), i.e. design the multiplier $\Pi \in \Pi_{pol}[\alpha_\phi, \beta_\phi]$, to reduce the computational cost associated with the evaluation of the neural network while preserving the stability of the perturbed feedback system.*

An implicit objective in solving Problem 1 is to characterize the "robust" region of attraction for the perturbed feedback system. Such a region of attraction corresponds to the set of all initial conditions $x(0) = x_0$ for which $x(k)$ converges to the equilibrium point x_* assuming that $\Delta \in \mathrm{IQC}(\Psi, M)$, i.e. $\lim_{k\to\infty} x(k) = x_*$, for all $\Delta \in \mathrm{IQC}(\Psi, M)$. As its characterization is not an easy task [27], we determine inner-approximations with a well-defined representation, such as ellipsoidal sets.

3.2 Design of the ETM Matrix

This section presents a solution to Problem 1. The proposed conditions are based on a multiplier $\Pi \in \Pi_{pol}[\alpha_\phi, \beta_\phi]$ with structure given by (16), (17), as studied in Section 2.3.

First of all, let us define the augmented state vector

$$\xi(k) = \begin{bmatrix}x(k)^\top & \psi(k)^\top\end{bmatrix}^\top \in \mathbb{R}^{n_\xi}, \tag{23}$$

with $n_\xi = n_G + n_\psi$. Thus, the dynamics of the perturbed system can be represented by the model:

$$\begin{aligned}\xi(k+1) &= \mathbb{A}\xi(k) + \mathbb{B}_u u(k) + \mathbb{B}_q q(k), \\ r(k) &= \mathbb{C}\xi(k) + \mathbb{D}_u u(k) + \mathbb{D}_q q(k),\end{aligned} \tag{24}$$

where

$$\begin{aligned}\mathbb{A} &= \begin{bmatrix}A_G & \mathbf{0} \\ B_{\Psi p}C_G & A_\Psi\end{bmatrix},\ \mathbb{B}_u = \begin{bmatrix}B_{Gu} \\ B_{\Psi p}D_{Gu}\end{bmatrix}, \\ \mathbb{B}_q &= \begin{bmatrix}B_{Gq} \\ B_{\Psi p}D_{Gq} + B_{\Psi q}\end{bmatrix},\ \mathbb{C} = \begin{bmatrix}D_{\Psi p}C_G & C_\Psi\end{bmatrix}, \\ \mathbb{D}_u &= D_{\Psi p}D_{Gu},\ \mathbb{D}_q = D_{\Psi p}D_{Gq} + D_{\Psi q}.\end{aligned} \tag{25}$$

We also denote the equilibrium $\xi_* = \begin{bmatrix}x_*^\top & \psi_*^\top\end{bmatrix}^\top$. Let us define the following useful matrices:

$$N_{u\xi} = \begin{bmatrix}N_{ux} & \mathbf{0}_{n_u \times n_\psi}\end{bmatrix}, R_{s\xi} = \left[\begin{array}{ccc}\mathbf{I}_{n_\xi} & \mathbf{0}_{n_\xi \times n_\phi} & \mathbf{0}_{n_\xi \times n_q} \\ \hline N_{u\xi} & N_{u\omega} & 0_{n_u \times n_q} \\ \mathbf{0}_{n_q \times n_\xi} & \mathbf{0}_{n_q \times n_\phi} & \mathbf{I}_{n_q}\end{array}\right],$$

$$N_{\nu\xi} = \begin{bmatrix}N_{\nu x} & \mathbf{0}_{n_\phi \times n_\psi}\end{bmatrix}, R_{\phi\xi} = \begin{bmatrix}N_{\nu\xi} & N_{\nu\omega} & \mathbf{0}_{n_\phi \times n_q} \\ \mathbf{0}_{n_\phi \times n_G} & \mathbf{I}_{n_\phi} & \mathbf{0}_{n_\phi \times n_q}\end{bmatrix},$$

$$\mathbb{W}^1_i = \begin{bmatrix}W^1_i & \mathbf{0}_{1 \times n_\psi}\end{bmatrix},$$

where W^1_i is the i^{th} row of W^1.

Theorem 1 *Consider the perturbed feedback system consisting of $\mathbb{G}(G, \Delta)$ in (1)-(9)-(11) and π_{ETM} in* (7)*-(8)-*(20)*. Let $\bar{\nu}^1 \in \mathbb{R}^{n_1}$, $\underline{\nu}^1 = 2\nu^1_* - \bar{\nu}^1$ and let $\underline{\nu}, \bar{\nu} \in \mathbb{R}^{n_\phi}$ be obtained from $\underline{\nu}^1$, $\bar{\nu}^1$ as described in Remark 1. Let $\alpha_\phi, \beta_\phi \in \mathbb{R}^{n_\phi}$ such that ϕ satisfies the local sector $\mathrm{sec}[\alpha_\phi, \beta_\phi]$ around the point ν_* restricted to the interval $[\underline{\nu}, \bar{\nu}]$. Assume that $\Delta \in IQC(\Psi, M)$ with Ψ and M known. If there exist a symmetric definite positive matrix $P_\xi \in \mathbb{R}^{n_\psi \times n_\psi}$, and a multiplier $\Pi = \Pi^\top \in \mathbb{R}^{2n_\phi \times 2n_\phi}$ as in* (16)*-*(17) *such that the inequalities (26) and*

$$\begin{bmatrix}(\bar{\nu}^1_i - \nu^1_{*,i})^2 & \mathbb{W}^1_i \\ \star & P_\xi\end{bmatrix} \geq \mathbf{0},\ i \in \{1, \ldots, n_1\}, \tag{27}$$

$$\begin{bmatrix}\mathbf{I}_{n_\phi} \\ \Lambda\end{bmatrix}^\top \Pi \begin{bmatrix}\mathbf{I}_{n_\phi} \\ \Lambda\end{bmatrix} \geq \mathbf{0},\ \forall \Lambda \in \mathtt{diag}([\alpha_\phi, \beta_\phi]), \tag{28}$$

$$\mathcal{H}_\xi := R_{s\xi}^\top \left(\left[\begin{array}{c|cc} \mathbb{A}^\top P_\xi \mathbb{A} - P_\xi & \mathbb{A}^\top P_\xi \mathbb{B}_u & \mathbb{A}^\top P_\xi \mathbb{B}_q \\ \hline \star & \mathbb{B}_u^\top P_\xi \mathbb{B}_u & \mathbb{B}_u^\top P_\xi \mathbb{B}_q \\ \star & \star & \mathbb{B}_q^\top P_\xi \mathbb{B}_q \end{array}\right] + \left[\begin{array}{c|cc} \mathbb{C} & \mathbb{D}_u & \mathbb{D}_q \end{array}\right]^\top M \left[\begin{array}{c|cc} \mathbb{C} & \mathbb{D}_u & \mathbb{D}_q \end{array}\right] \right) R_{s\xi} + R_{\phi\xi}^\top \Pi R_{\phi\xi} < \mathbf{0}, \quad (26)$$

hold then: i) *the closed-loop system is locally asymptotically stable around* ξ_* *for any* $\Delta \in IQC(\Psi, M)$, *and* ii) *the set* $\mathcal{E}(P_\xi, \xi_*) = \{\xi \in \mathbb{R}^{n_\xi} : (\xi - \xi_*)^\top P_\xi (\xi - \xi_*) \leq 1\}$ *is an estimate of its region of attraction.*

Proof. First, suppose that (28) is feasible, then it follows that $\Pi \in \Pi_{pol}[\alpha_\phi, \beta_\phi]$ and therefore Lemma 2 applies. Secondly, (27) guarantees that $\nu^1(k) \in [\underline{\nu}^1, \bar{\nu}^1]$ and thus the conclusion of Lemma 3 holds. From this point, the proof leverages that one of Theorem 2 in [33] where ω_ϕ and $\Psi_\phi^\top M_\phi(\lambda)\Psi_\phi$ are replaced by $\hat{\omega}_\phi$ and Π, respectively. Furthermore, since [33] defines the augmented system (24) in a more compact form, it is necessary to consider the partitioning of the blocks indicated by the gray lines in (26) to make the correspondences between both approaches. □

Remark 3 *For a particular perturbation* Δ, *there exists a class of valid time-domain IQCs defined by a fixed filter* Ψ *and a matrix* M *taken from a constraint set* $\mathcal{M}$ *[29, Class 12]. Consequently, the matrix* $M \in \mathcal{M}$ *can be treated as an additional variable to reduce conservatism.*

Remark 4 *By considering in the top left block of (26),* $\mathbb{A}^\top P_\xi \mathbb{A} - \lambda P_\xi$, *with* $\lambda \in (0, 1)$ *a new decision variable, instead of* $\mathbb{A}^\top P_\xi \mathbb{A} - P_\xi$, *the exponential convergence with rate* λ *is obtained.*

Theorem 1 can be simplified to handle unperturbed systems, that is, system (1) defined by:

$$x(k+1) = A_G x(k) + B_G u(k). \quad (29)$$

Corollary 1 *Consider the feedback system consisting of* G *in (29) and* π_{ETM} *in* (7)*-(8)-*(20). *Let* $\bar{\nu}^1 \in \mathbb{R}^{n_1}$, $\underline{\nu}^1 = 2\nu_*^1 - \bar{\nu}^1$ *and let* $\underline{\nu}, \bar{\nu} \in \mathbb{R}^{n_\phi}$ *be obtained from* $\underline{\nu}^1$, $\bar{\nu}^1$ *as described in Remark 1. Let* $\alpha_\phi, \beta_\phi \in \mathbb{R}^{n_\phi}$ *such that* ϕ *satisfies the local sector* $\text{sec}[\alpha_\phi, \beta_\phi]$ *around the point* ν_* *restricted to the interval* $[\underline{\nu}, \bar{\nu}]$. *If there exist a symmetric definite positive matrix* $P \in \mathbb{R}^{n_G \times n_G}$, *and a multiplier* $\Pi = \Pi^\top \in \mathbb{R}^{2n_\phi \times 2n_\phi}$ *as in* (16)-(17) *such that the following inequalities hold*

$$\mathcal{H} := R_s^\top \begin{bmatrix} A_G^\top P A_G - P & A_G^\top P B_G \\ \star & B_G^\top P B_G \end{bmatrix} R_s + R_\phi^\top \Pi R_\phi < \mathbf{0}, \quad (30)$$

$$\begin{bmatrix} (\bar{\nu}_i^1 - \nu_{*,i}^1)^2 & W_i^1 \\ \star & P \end{bmatrix} \geq \mathbf{0}, \ i \in \{1, \ldots, n_1\}, \quad (31)$$

$$\begin{bmatrix} \mathbf{I}_{n_\phi} \\ \Lambda \end{bmatrix}^\top \Pi \begin{bmatrix} \mathbf{I}_{n_\phi} \\ \Lambda \end{bmatrix} > \mathbf{0}, \ \forall \Lambda \in \texttt{diag}([\alpha_\phi, \beta_\phi]), \quad (32)$$

where

$$R_s = \begin{bmatrix} I_{n_G} & 0_{n_G \times n_\phi} \\ N_{ux} & N_{u\omega} \end{bmatrix}, \ R_\phi = \begin{bmatrix} N_{\nu x} & N_{\nu\omega} \\ 0_{n_\phi \times n_G} & I_{n_\phi} \end{bmatrix}$$

then: i) *the closed-loop system is locally asymptotically stable around* x_*, *and* ii) *the set* $\mathcal{E}(P, x_*) = \{x \in \mathbb{R}^{n_G} : (x - x_*)^\top P (x - x_*) \leq 1\}$ *is an estimate of the region of attraction for the feedback system.*

Proof. First, suppose that (32) is feasible, then Lemma 2 applies. Secondly, (31) guarantees that $\nu^1(k) \in [\underline{\nu}^1, \bar{\nu}^1]$ and thus the conclusion of Lemma 3 holds. From this point, the proof is similar to that of Theorem 1 in [33] where ω_ϕ and $\Psi_\phi^\top M_\phi(\lambda)\Psi_\phi$ are replaced by $\hat{\omega}_\phi$ and Π, respectively. □

Remark 5 *Conditions of Theorem 1 and Corollary 1 involve an infinite number of LMIs in* (28) *and* (32). *However, as already mentioned in Section 2.3, they can be reduced to a finite number of LMIs by constraining block* Z *in the* Π *matrix to have nonpositive diagonal elements. In that case [33], the conditions* (28) *and* (32) *need only to be checked at the vertices of the matrix interval* $\texttt{diag}([\alpha_\phi, \beta_\phi])$.

Based on (20), the greater is the local sector $\text{sec}[\alpha_\phi, \beta_\phi]$, the lower is the evaluation activity in the neural network. Therefore, we are interested in finding the largest sector that results in feasible conditions. Furthermore, as it is well-known that there is a trade-off between the update saving and the size of the estimate of the region of attraction (see, e.g., [2]), it seems reasonable to propose an optimization function that can help to enlarge such an estimate, while reducing the amount of computation. Given the sector bounds α_ϕ and β_ϕ, the following optimization is considered:

$$\mathcal{O} : \begin{cases} \min \ \rho, \\ \text{s.t.} \ \ (26), (27), (28), \mathcal{H}_\xi \geq -\rho I_{n_\xi + 2n_\phi + n_q} \end{cases} \quad (33)$$

From (26), we want the matrix $\mathcal{H}_\xi$ to be as close as possible to zero. Thus, for a given local sector $\text{sec}[\alpha_\phi, \beta_\phi]$,

we are indirectly 1) minimizing P_ξ, consequently maximizing the estimate of the region of attraction, and 2) approaching the infeasibility of the stability condition related to the values α_ϕ and β_ϕ. In the case of Corollary 1, the constraints of the optimization problem (33) are changed by (30), (31), (32) and $\mathcal{H} \geq -\rho \mathbf{I}_{n_G+2n_\phi}$.

4 Simulations

Consider the nonlinear inverted pendulum system with mass $m = 0.15\ kg$, length $l = 0.5\ m$, and friction coefficient $\mu = 0.5\ Nms/rad$. Its dynamics is described by the following model

$$\dot{x}(t) = \begin{bmatrix} 0 & 1 \\ \frac{g}{l} & -\frac{\mu}{ml^2} \end{bmatrix} x(t) + \begin{bmatrix} 0 \\ \frac{1}{ml^2} \end{bmatrix} u(t) + \begin{bmatrix} 0 \\ -\frac{g}{l} \end{bmatrix} q(t), \tag{34}$$

where the plant state is $x(t) = \begin{bmatrix} \theta(t) & \dot{\theta}(t) \end{bmatrix}^\top$ with $\theta(t)$ the angular position (rad), the control input is $u(t)$, and the static non-linearity is $q(t) = \theta(t) - \sin(\theta(t))$. The system is discretized with a sampling time $dt = 0.02$ seconds. To stabilize it, we have designed a controller in the same way as in [33]. Such a controller is parameterized by a 2-layer feedforward neural network with $n_1 = n_2 = 32$, $tanh$ is the activation function for both layers and $b^i = \mathbf{0}$, $i \in \{1, 2, 3\}$, ensuring that the equilibrium point is at the origin, i.e. $(x_*, u_*, \nu_*, \omega_*, p_*, q_*) = \mathbf{0}$. Also, $0 = \Delta(0)$ for all $\Delta \in IQC(\Psi, M)$. Consequently, the perturbation's internal state also has zero initial condition.

With respect to the perturbation, we assume that $\Delta \in IQC(\Psi, M)$. Then according to Definition 1 and definition of Ψ in (10), one considers:

$$\Psi = \left[\begin{array}{c|cc} 0 & -L_s & \mathbf{I} \\ \hline \mathbf{I} & L_s & -\mathbf{I} \\ 0 & -m_s & \mathbf{I} \end{array}\right] \text{ and } M = \begin{bmatrix} 0 & M_{12} \\ \star & 0 \end{bmatrix}, \tag{35}$$

where $L_s = (\bar{\theta} - \sin(\bar{\theta}))/\bar{\theta}$, $\bar{\theta} = 0.73$, $m_s = 0$, and $M_{12} \geq 0$ is a matrix to be designed.

To illustrate the efficiency of the proposal, let us first consider $\Pi = \Pi_{ds}$. Our first goal is to evaluate the influence of the size of the local sector $\text{sec}[\alpha_\phi, \beta_\phi]$ on the transmission activity in the neural network. To do this, we solve the optimization procedure (33) for some increasing α_ϕ and β_ϕ bounds. To compute the lower bounds α_ϕ, we impose different constraints on $\nu^1 \in [\underline{\nu}^1, \bar{\nu}^1]$, $\bar{\nu}^1 = -\underline{\nu}^1 = \delta_\alpha \times \mathbf{1}_{32\times 1}$. The notation $\alpha_\phi|_{\delta_\alpha}$ will be used to indicate the values of α_ϕ calculated from δ_α. The upper bounds are directly selected from the unity, i.e. $\beta_\phi = \delta_\beta \times \mathbf{1}_{64\times 1}$. For each case, we simulate the feedback system response for 100 initial conditions belonging to the domain of attraction. By defining the update rate r_i of the i^{th} layer as the ratio between its number of events and the number of samplings, Table 1 shows r_1 and r_2 for different local sectors $\text{sec}[\alpha_\phi, \beta_\phi]$. Also, in the fourth column of both tables, we put a measure of the income of the ETMs. As we can see, in general, the bigger is the local sector $\text{sec}[\alpha_\phi, \beta_\phi]$, the lower is the update rate of the layers. Such a reduction become more pronounced when we enlarge β_ϕ.

Local sector bounds	Update rate (%)			Area
	r_1	r_2	$\frac{r_1+r_2}{2}$	
$\alpha_\phi\|_{\delta_\alpha=0.2}, \beta_\phi = \mathbf{1}_{64\times 1}$	99.68	99.25	99.46	0.92
$\alpha_\phi\|_{\delta_\alpha=0.3}, \beta_\phi = \mathbf{1}_{64\times 1}$	99.46	98.91	99.19	2.29
$\alpha_\phi\|_{\delta_\alpha=0.4}, \beta_\phi = \mathbf{1}_{64\times 1}$	99.30	98.56	98.93	4.54
$\alpha_\phi\|_{\delta_\alpha=0.2}, \beta_\phi = 1.025 \times \mathbf{1}_{64\times 1}$	45.37	38.88	42.12	0.89
$\alpha_\phi\|_{\delta_\alpha=0.3}, \beta_\phi = 1.025 \times \mathbf{1}_{64\times 1}$	39.46	38.98	39.22	2.22
$\alpha_\phi\|_{\delta_\alpha=0.4}, \beta_\phi = 1.025 \times \mathbf{1}_{64\times 1}$	39.36	38.52	38.94	4.39
$\alpha_\phi\|_{\delta_\alpha=0.2}, \beta_\phi = 1.05 \times \mathbf{1}_{64\times 1}$	49.00	22.14	35.57	0.86
$\alpha_\phi\|_{\delta_\alpha=0.3}, \beta_\phi = 1.05 \times \mathbf{1}_{64\times 1}$	37.66	21.92	29.79	2.14
$\alpha_\phi\|_{\delta_\alpha=0.4}, \beta_\phi = 1.05 \times \mathbf{1}_{64\times 1}$	32.28	21.88	27.08	4.25

Table 1
Comparison of updates rate for different local sectors.

In addition, we investigate the influence of the size of the local sector $\text{sec}[\alpha_\phi, \beta_\phi]$ on the size of the estimate of the region of attraction. In this case, we compute the area of the ellipses resulting from the projection of the ellipsoid $\mathcal{E}(P_\xi, \xi_*)$ with the plane formed by the plant states $(x_1 \times x_2)$ for each local sector considered in the last case. The results are shown in the last column of Table 1. Note that the ellipses increase when α_ϕ bounds increase, which is reasonable, since we have larger ν^1 bounds. On the other hand, the ellipses slightly decreases when β_ϕ bounds increase, which can be related to the trade-off mentioned earlier. This can also be verified in Figure 2.

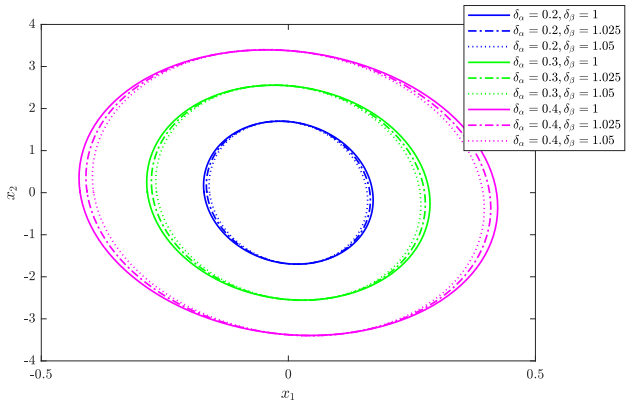

Fig. 2. Projection of $\mathcal{E}(P_\xi, \xi_*)$ on the plane $x_1 \times x_2$ for local sectors given by $\alpha_\phi|_{\delta_\alpha}$ and $\beta_\phi = \delta_\beta \times \mathbf{1}_{64\times 1}$.

By considering the largest local sector (last line in Ta-

ble 1), we plot the closed-loop system temporal response for an initial condition belonging to the domain of attraction. Figure 3 shows the plant states (top) and the control input (bottom), where we can verify the convergence of the trajectories to the origin in both cases. The intervals between events of the layers ω^1 (magenta solid lines) and ω^2 (cyan dashed point lines) are presented in Figure 4. In this case, we have found update rates of 33.80% and 21.60% for ω^1 and ω^2, respectively. Therefore, by introducing ETMs on the output of the layers, we were able to reduce 72.30% of the transmission activity on the neural network. This have a direct impact on the computational cost associated with the evaluation of the control law.

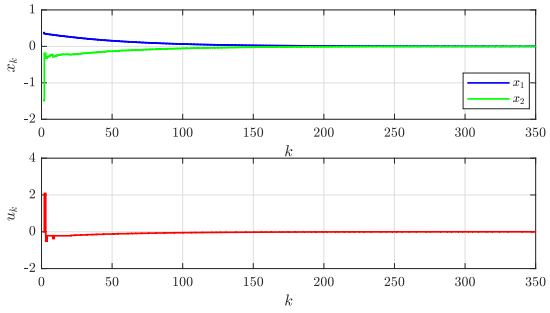

Fig. 3. The closed-loop system response for $x(0) = \begin{bmatrix} 0.3758 & -1.4850 \end{bmatrix}^\top$.

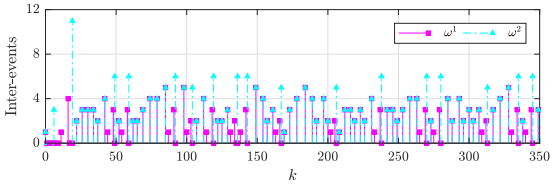

Fig. 4. Inter-events of the layers ω^1 and ω^2.

Furthermore, to verify the reduction of the evaluation activity for a neural network with more layers/neurons, we designed two other controllers, one with 3 layers $n_1 = n_2 = n_3 = 32$ and another with 4 layers $n_1 = n_2 = n_4 = 32$ and $n_3 = 16$. For the first one we solved the optimization procedure (33) with $\alpha_\phi|_{\delta_\alpha=0.15}$ and $\beta_\phi = 1.05 \times \mathbf{1}_{96\times 1}$, and for the second one, we considered $\alpha_\phi|_{\delta_\alpha=0.04}$ and $\beta_\phi = 1.05 \times \mathbf{1}_{112\times 1}$. The update rate obtained for each layer of each controller is shown in Table 2. Note that for both controllers, the evaluation activity has been approximately halved.

Now we consider Π given by (16)-(17). By repeating the same simulations as before, we have found the update rates shown in Table 3. For the 2-layers controller, we used $\alpha_\phi|_{\delta_\alpha=0.4}$ and $\beta_\phi = 1.05 \times \mathbf{1}_{64\times 1}$, and for the others, the same values indicated in the previous paragraph. Note that, with this general multiplier, we have further

ℓ	Update rate (%)					Area
	r_1	r_2	r_3	r_4	$\frac{\sum_{i=1}^{\ell} r_i}{\ell}$	
3	51.18	50.99	50.48	-	50.88	5.33
4	50.51	48.18	48.02	47.95	48.67	0.14

Table 2
The update rates for the NN controllers with 3 and 4 layers.

reduced the transmission activity on the neural network for the 2 and 3-layers controllers. On the other hand, for the 4-layers controller, the percentage of transmission remained almost the same. In addition, we have put in the last column of Table 3, the area of the projection of $\mathcal{E}(P_\xi, \xi_*)$ on the plane $(x_1 \times x_2)$ obtained. Comparing with the results of tables 1 and 2, we can see that bigger regions are estimated using Π.

ℓ	Update rate (%)					Area
	r_1	r_2	r_3	r_4	$\frac{\sum_{i=1}^{\ell} r_i}{\ell}$	
2	27.33	21.75	-	-	24.54	7.87
3	38.45	16.28	15.29	-	23.34	5.58
4	48.65	48.33	48.33	48.26	48.39	0.34

Table 3
Percentage of updates for NNs with 3 and 4 layers.

5 Conclusion

This paper proposed a novel event-triggering strategy, based on (local) sectors conditions related to the activation functions in order to decide whether the outputs of the layers should be transmitted through the network or not. Theoretical conditions allowed to design the event-triggering mechanism and to estimate the region of attraction, while preserving the stability and suitable performance of the closed-loop system. Simulations have illustrated the effectiveness of the event-triggering scheme, showing a significant reduction of the transmission activity in the neural network even if the number of layer increase. The results open the doors for future works as studying other event-triggering structures and different abstractions in order to reduce the conservatism of the conditions.

References

[1] C. De Souza, V. J. S. Leite, S. Tarbouriech, E. B. Castelan, and L. F. P. Silva. A direct parameter-error co-design approach of discrete-time saturated LPV systems. *IEEE Transactions on Automatic Control*, 2022.

[2] C. de Souza, V.J.S. Leite, S. Tarbouriech, and E.B. Castelan. Event-triggered policy for DOF stabilization of discrete-time LPV systems under input constraints. *System & Control Letters*, 153:104950, 2020.

[3] C. de Souza, S. Tarbouriech, and A. Girard. Event-triggered neural network control for LTI systems. *IEEE Control Systems Letters*, 7:1381–1386, 2023.

[4] D. V. Dimarogonas and K. H. Johansson. Event-triggered control for multi-agent systems. In *Proceedings of the 48h IEEE Conference on Decision and Control (CDC) held jointly with 2009 28th Chinese Control Conference*, pages 7131–7136. IEEE, 2009.

[5] Y. Ebihara, H. Waki, V. Magron, N. H. A. Mai, D. Peaucelle, and S. Tarbouriech. Stability analysis of recurrent neural networks by IQC with copositive mutipliers. In *60th IEEE Conference on Decision and Control (CDC)*, pages 5098–5103. IEEE, 2021.

[6] M. Fazlyab, M. Morari, and G. J. Pappas. Safety verification and robustness analysis of neural networks via quadratic constraints and semidefinite programming. *IEEE Transactions on Automatic Control*, 2020.

[7] M. Fazlyab, A. Robey, H. Hassani, M. Morari, and G. Pappas. Efficient and accurate estimation of Lipschitz constants for deep neural networks. *Advances in Neural Information Processing Systems*, 32, 2019.

[8] M. Fetzer and C. W. Scherer. Absolute stability analysis of discrete time feedback interconnections. *IFAC-PapersOnLine*, 50(1):8447–8453, 2017.

[9] Y. Gao, X. Guo, R. Yao, W. Zhou, and C. Cattani. Stability analysis of neural network controller based on event triggering. *Journal of the Franklin Institute*, 357(14):9960–9975, 2020.

[10] A. Girard. Dynamic triggering mechanisms for event-triggered control. *IEEE Transactions on Automatic Control*, 60(7):1992–1997, 2014.

[11] W. P. M. H. Heemels, M. C. F. Donkers, and A. R. Teel. Periodic event-triggered control for linear systems. *IEEE Transactions on Automatic control*, 58(4):847–861, 2012.

[12] W. P. M. H. Heemels, J. H. Sandee, and P. P. J. Van Den Bosch. Analysis of event-driven controllers for linear systems. *International Journal of Control*, 81(4):571–590, 2008.

[13] M. Hertneck, J. Köhler, S. Trimpe, and F. Allgöwer. Learning an approximate model predictive controller with guarantees. *IEEE Control Systems Letters*, 2(3):543–548, 2018.

[14] B. Hu, M. J. Lacerda, and P. Seiler. Robustness analysis of uncertain discrete-time systems with dissipation inequalities and integral quadratic constraints. *International Journal of Robust and Nonlinear Control*, 27(11):1940–1962, 2017.

[15] M. Jin and J. Lavaei. Stability-certified reinforcement learning: A control-theoretic perspective. *IEEE Access*, 8:229086–229100, 2020.

[16] B. Karg and S. Lucia. Efficient representation and approximation of model predictive control laws via deep learning. *IEEE Transactions on Cybernetics*, 50(9):3866–3878, 2020.

[17] H. K. Khalil. *Nonlinear control*, volume 406. Pearson New York, 2015.

[18] K.-K. K. Kim, E. R. Patrón, and R.D. Braatz. Standard representation and unified stability analysis for dynamic artificial neural network models. *Neural Networks*, 98:251–262, 2018.

[19] A. Megretski and A. Rantzer. System analysis via integral quadratic constraints. *IEEE Transactions on Automatic Control*, 42(6):819–830, 1997.

[20] P. Pauli, A. Koch, J. Berberich, P. Kohler, and F. Allgöwer. Training robust neural networks using Lipschitz bounds. *IEEE Control Systems Letters*, 6:121–126, 2021.

[21] P. Pauli, J. Köhler, J. Berberich, A. Koch, and F. Allgöwer. Offset-free setpoint tracking using neural network controllers. In *Learning for Dynamics and Control*, pages 992–003. PMLR, 2021.

[22] M. Revay, R. Wang, and I. R. Manchester. Lipschitz bounded equilibrium networks. *arXiv preprint arXiv:2010.01732*, 2020.

[23] A. Sahoo, H. Xu, and S. Jagannathan. Neural network-based event-triggered state feedback control of nonlinear continuous-time systems. *IEEE Transactions on Neural Networks and Learning Systems*, 27(3):497–509, 2015.

[24] P. Seiler. Stability analysis with dissipation inequalities and integral quadratic constraints. *IEEE Transactions on Automatic Control*, 60(6):1704–1709, 2014.

[25] P. Tabuada. Event-triggered real-time scheduling of stabilizing control tasks. *IEEE Transactions on Automatic Control*, 52(9):1680–1685, 2007.

[26] K. Tanaka. An approach to stability criteria of neural-network control systems. *IEEE Transactions on Neural Networks*, 7(3):629–642, 1996.

[27] S. Tarbouriech, G. Garcia, J. M. Gomes da Silva Jr., and I. Queinnec. *Stability And Stabilization Of Linear Systems With Saturating Actuators*. Springer, 2011.

[28] K. G. Vamvoudakis. Event-triggered optimal adaptive control algorithm for continuous-time nonlinear systems. *IEEE/CAA Journal of Automatica Sinica*, 1(3):282–293, 2014.

[29] J. Veenman, C. W. Scherer, and H. Köroğlu. Robust stability and performance analysis based on integral quadratic constraints. *European Journal of Control*, 31:1–32, 2016.

[30] B. Widrow and M. A. Lehr. 30 years of adaptive neural networks: perceptron, madaline, and backpropagation. *Proceedings of the IEEE*, 78(9):1415–1442, 1990.

[31] W. Wu, S. Reimann, and S. Liu. Event-triggered control for linear systems subject to actuator saturation. *IFAC Proceedings Volumes*, 47(3):9492–9497, 2014.

[32] L. Xing, C. Wen, Z. Liu, H. Su, and J. Cai. Event-triggered adaptive control for a class of uncertain nonlinear systems. *IEEE Transactions on Automatic Control*, 62(4):2071–2076, 2016.

[33] H. Yin, P. Seiler, and M. Arcak. Stability analysis using quadratic constraints for systems with neural network controllers. *IEEE Transactions on Automatic Control*, 2021.

[34] X. Zhang, M. Bujarbaruah, and F. Borrelli. Safe and near-optimal policy learning for model predictive control using primal-dual neural networks. In *American Control Conference (ACC)*, pages 354–359. IEEE, 2019.

[35] X. Zhong, Z. Ni, H. He, X. Xu, and D. Zhao. Event-triggered reinforcement learning approach for unknown nonlinear continuous-time system. In *International Joint Conference on Neural Networks (IJCNN)*, pages 3677–3684. IEEE, 2014.